Int. J. Nonlinear Anal. Appl. 14 (2023) 1, 2301–2312
ISSN: 2008-6822 (electronic)
http://dx.doi.org/10.22075/ijnaa.2022.28910.4020

A mathematical study of nanoparticle aided hyperthermia treatment of hepatic cancer using magnetite nanoparticles under alternating and rotating magnetic fields

Faizan Ahmad Zargar[a,*], Mukhtar Ahmad Khanday[a], Mudasir Ashraf[b,c]

[a]*Department of Mathematics, University of Kashmir, Srinagar - 190006, J&K, India*

[b]*Radiological Physics, Department of Radiodiagnosis, JNMC, Aligarh Muslim University, Aligarh - 202002, U.P, India*

[c]*Department of Radiological Physics & Bio-Engineering, SKIMS, Srinagar - 190011, J&K, India*

(Communicated by Javad Damirchi)

Abstract

Hyperthermia is a method of cancer treatment wherein the temperature of the tumor is increased to over 315 K (42°C) for a specific duration, ultimately leading to cell death by inducing apoptosis or necrosis. Magnetic Particle Hyperthermia (MPH) is a non-invasive method of cancer treatment in which magnetic nanoparticles are introduced to the tumor at its center and are then subject to a magnetic field. Magnetic nanoparticles upon being exposed to a magnetic field exhibit a heating effect by conversion of magnetic field energy into heat energy. Owing to high acidity, tumor cells are more sensitive to heating than healthy cells, thus if the tumor is heated to 315-319K (42°–46° C), it will be destroyed with minimal to no damage to healthy tissues surrounding the tumor. During the application of hyperthermia as a cancer treatment, blood perfusion protects the healthy tissues surrounding the tumor region from damage due to heat by dissipating any excess heat. In this paper, the temperature profiles were estimated inside a presumably spherical hepatic tumor mass by solving Pennes' Bio-heat Equation containing the power term. The results were obtained using analytic as well as numerical methods using MPH with mineral oil as a carrier liquid and Magnetite (Fe_3O_4) nanoparticles with a mean diameter of 10.9 nm subject to Alternating Magnetic Field (AMF) and Rotating Magnetic Field (RMF).

Keywords: Magnetic Particle Hyperthermia, hepatic cancer treatment, Pennes' Bioheat Equation, medical hyperthermia
2020 MSC: 92B05, 92C05, 92C50

1 Introduction

Hyperthermia is the state of a living tissue or an organ in which its temperature gets raised to abnormally high temperatures. In medical usage this has been modified to treat various types of cancers with an advantage of being non invasive over surgical ablation and also proving very useful for treatment of inoperable areas of the body [8].

*Corresponding author
Email addresses: faizanzgr@gmail.com (Faizan Ahmad Zargar), khanday@uok.edu.in (Mukhtar Ahmad Khanday), mudasirashraf8@gmail.com (Mudasir Ashraf)

Received: November 2022 *Accepted:* December 2022

During the application of hyperthermia treatment, the temperature of the target tissue is increased to over 315 K (42°C) for a specific duration, ultimately leading to cell death by inducing apoptosis or necrosis, as the living cells cannot survive temperatures exceeding 315 K (42°C).

Hepatic cancer is one of the major causes of death due to cancers worldwide and its onset is mainly caused by Hepatitis B or C Virus, alcohol consumption, fatty liver disease, etc. Hepatocellular carcinoma (HCC) is the most common hepatic cancer found in adults. Hepatocellular carcinoma (HCC) has been classified into various subtypes, the most important being fibrolamellar carcinoma. It is very rare, usually seen in women aged 35 years or more and provides a better outlook of the Hepatocellular carcinoma (HCC). Marina Galicia-Moreno et al., [8] reviewed first and second line treatments of Hepatocellular carcinoma (HCC). Dev Kumar et al, [3] discussed the formulations of superparamagnetic iron oxide, gold nanorods and nanoshells, and carbon nanotubes for magnetic nanoparticle hyperthermia. Vahid Darvishi et al., [6] developed a method for analysing drug delivery and distribution of magnetic nanoparticles in fluid hyperthermia cancer treatment and illustrated that the effect of distribution of nanoparticles in the treatment.

Magnetic fluids placed in a magnetic field generate heat by converting magnetic field energy into heat energy. The intensity of the heat generated by this conversion depends on various parameters relating to the magnetic field such as frequency and amplitude as well as the composition of the magnetic fluid (distribution of the particle size, type of particles, carrier liquid, surface-active agent, etc.). The behaviour of magnetic fluid exposed to magnetic fields has been studied since long leading to its application in medical science though still under development for overcoming the limitation of heating the target tissue to the maximum temperature with minimal to no damage to the surrounding healthy tissue [18]. Vicky V. Mody et al. [17] reviewed the dependence of magnetic properties of the nanoparticles on their shape, size, surface coating and doping, and maintained the clinical status of magnetic nanoparticles for the application of magnetic fluid hyperthermia. Lacis [15] in 1999 attempted to study the fluid movement at some specific frequencies of applied magnetic field. Zakinyan et al. [25] studied the behavior of a drop of kerosene based magnetic fluid composed of magnetite nanoparticles of size 10 nm surrounded by a nonmagnetic liquid on a solid horizontal surface under the action of a low frequency ($\simeq$ 1 Hz) uniform Rotating Magnetic Field (RMF). Dieckhoff et al. [7] used phase-lag research to study the behaviour of magnetic nanoparticles exposed to Rotating Magnetic Field (RMF) and Alternating Magnetic Field (AMF) at low frequencies. The dynamic behavior of particles in a magnetic field is also explainable by solutions Fokker–Planck equations as studied in detail by Yoshida T, et al., [24] using numerical simulation to clarify various dynamic properties including the M-H curve and field dependent relaxation time. Miloš Beković, et al. [2] proposed a new measuring system for characterising the magnetic flux losses systematically and generated a high frequency Rotating Magnetic Field (RMF) with adequate amplitudes suitable for making hyperthermia applicable in medical science.

Magnetic fluid hyperthermia induces heat conversion from magnetic nanoparticles by magnetic energy loss when subject to a magnetic field such as the Alternating Magnetic Field (AMF) or the Rotating Magnetic Field (RMF). This heat produced gets transmitted to the surrounding target tissue, thereby raising its temperature and is sufficient to cause damage to the cancer cells by necrosis and apoptosis, hence destroying the tumor.

Necrosis occurs in cells due to high exposure to extreme conditions that vary from the normal conditions causing damage to the internal cellular environment which results in rapid cell and tissue damage. It is a passive and unprogrammed cell death.

Apoptosis is a programmed cell death (PCD) that regulates and controls the growth and development of an organism. It is also known as cellular suicide, as in this process, the cell itself takes part in its death by shrinking, drying, condensing and finally fragmenting.

Both the above processes of cell death are depicted with a diagram in ***Figure 1*** below.

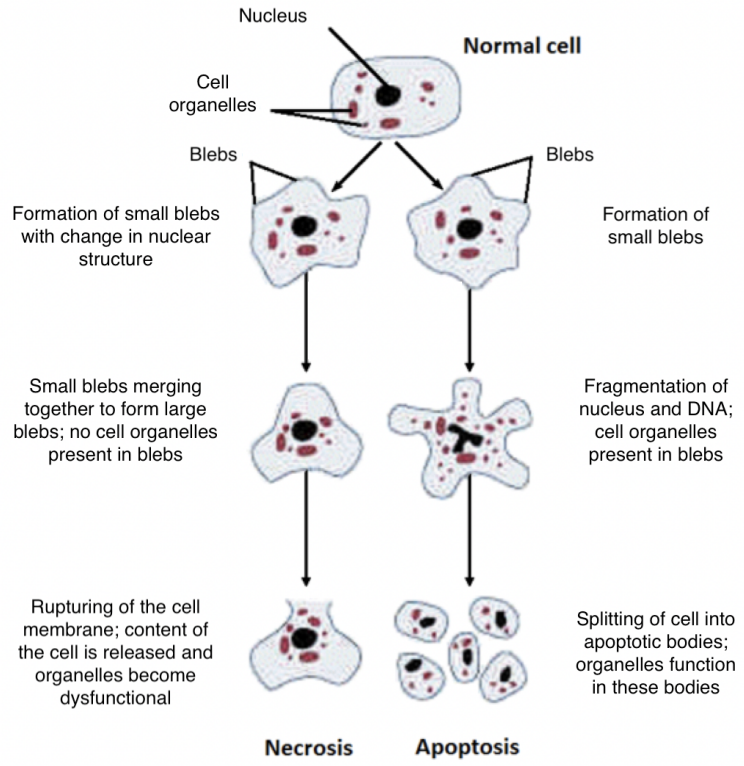

Figure 1: Processes of cell death [19]

Magnetic nanoparticles are delivered to the tumor through direct injection into the tumor region. After the delivery of magnetic nanoparticles, an alternating magnetic field or a rotating magnetic field is applied to generate heat in the nanoparticles through an energy conversion based on the principle of the hysteresis loss or the Néelian and Brownian relaxation. Eventually, this heat generated due hysteresis loss gets dissipated into the surrounding tumor tissue, thereby increasing its temperature which ultimately leads to cell death [10].
In this paper we consider a host with primary hepatic cancer and approximate the tumor mass to a sphere as shown in ***Figure 2*** with Gaussian heat source magnetic fluid ***Figure 3*** under applied magnetic fluid hyperthermia consisting of Magnetite nanoparticles under Alternating Magnetic Field (AMF) and Rotating Magnetic Field (RMF).

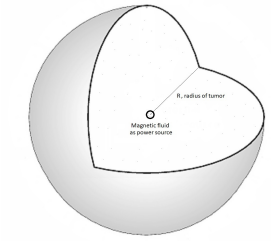

Figure 2: Spherical approximation of tumor mass

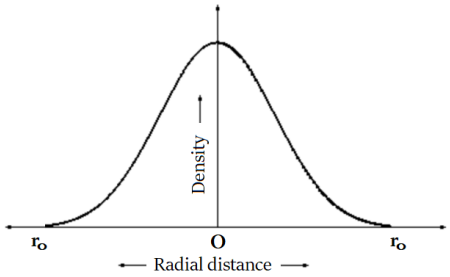

Figure 3: Gaussian distributed source

2 Methods

Magnetic relaxation of a single domain magnetic nanoparticle suspended in a fluid is explained by Brownian Relaxation [11] and Néel Relaxation [11] theories.

Magnetic relaxation is a measure of the tendency of a magnetic system to maintain equilibrium or a steady-state condition upon a change in the magnetic field. The characteristic times that are required to reach this equilibrium are known as relaxation times. Néel relaxation is caused by magnetisation vector reorientation against an energy barrier inside the nanoparticle magnetic core. [22] while Brownian relaxation is a result of rotational diffusion of the magnetic nanoparticle as a whole in the carrier liquid. [22]
The Nél and Brownian relaxation times, τ_N and τ_B [11], are given by;

$$\tau_N = \tau_0 \exp\left(\frac{K_U V_M}{k_b T}\right) \tag{2.1}$$

$$\tau_B = \frac{3\eta V_H}{k_b T} \tag{2.2}$$

where τ_0, K_U, V_M, k_b, T, η, and $V_H = (\frac{1+2\delta}{D})^3 V_M$ are the characteristic time constant ($=10^{-9}$), anisotropy constant, primary volume of the MNPs, Boltzmann constant, temperature, viscosity of the solvent, and hydrodynamic volume of the MNPs, respectively and δ is the thickness ($= 10^{-9}$ m) of sorbed layer of the surfactant. It was put forward by Rosensweig that Néel and Brownian relaxations occur in parallel [22], with an effective relaxation angular frequency as an inverse of effective relaxation time, given by;

$$\omega_{eff} = \frac{1}{\tau} = \frac{1}{\tau_N} + \frac{1}{\tau_B} \tag{2.3}$$

For an adequately large magnetic field strength, the Néel relaxation time can change by a number of orders of magnitude, whereas the Brownian relaxation time is appositely insensitive to the strength of the applied magnetic field and hence the Néel mechanism of relaxation also plays a very significant role. Miloš Beković, et al. [2] gave the modified expression for power dissipation that takes into account the thermal relaxation of the (restricted case) linear response theory given by;

$$P_0 = \mu_0 \pi \chi_0 f {H_0}^2 \left(\frac{2\pi f\tau}{1+(2\pi f\tau)^2}\right) \tag{2.4}$$

where μ_0 denotes the magnetic permeability of the free space, χ_0 – the equilibrium susceptibility, f and H_0 – the frequency and the amplitude of Alternating Magnetic Field (AMF) and $\chi = \chi_i \frac{3}{\zeta}(\coth\zeta - \frac{1}{\zeta})$ where $\chi_i = \frac{\mu_0 \phi M_d^2 V_M}{3 k_B T}$, $\zeta = \frac{\mu_0 M_d H V_M}{k_B T}$, $H = H_0 \cos(2\pi f t)$, M_d is the domain magnetization of a suspended particle, and $V_M = \frac{\pi}{6} D^3$.

Power Loss P_0 in the RMF is calculated using the following equation [2];

$$P_0 = \mu_0 \frac{2\pi f}{2}(m_x H_x + m_y H_y) \tag{2.5}$$

where H_x and H_y represent magnetic field strengths along $x - direction$ and $y - direction$ respectively, $2\pi f$ is the angular frequency, m_x and m_y are the resolved magnetisation components of the magnetic field along x- direction and y-direction respectively. ***Figure 4*** and ***Figure 5*** shows the coil arrangement for AMF and RMF respectively.

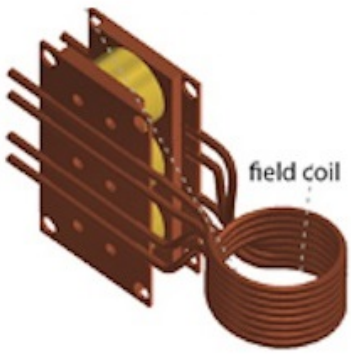

Figure 4: Coil arrangement for AMF [5]

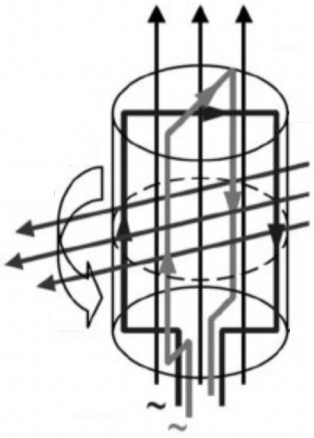

Figure 5: Coil arrangement for RMF [14]

As the temperature of the tissue increases, the excess heat generated is dissipated by the mechanism of thermoregulation of the body by increasing the blood flow to the tumor region. In response to temperature rise, the blood flow rate inside the healthy tissues of the body that surround the tumor increases many folds, while inside the tumor, the blood flow rate increases only up to twice its normal flow rate, thus protecting the healthy tissues up to a specific point. [9].

2.1 Governing Equation

The equation governing heat transfer in biological tissues is a partial differential equation which was put forward by H.H. Pennes [20] as given below;

$$\rho_p c_p \frac{\partial T}{\partial t} = \nabla \cdot (k \nabla T) + \rho_b c_b \omega_b (T_a - T) + Q \tag{2.6}$$

where ρ_p and c_p are the density and specific heat capacity of the tumor mass, k is the thermal conductivity, ρ_b and c_b the density and specific heat capacity of blood, ω_b the blood perfusion rate, T_a the arterial blood temperature, Q the constant heat generation due to metabolism.

Its modified radial form that includes a power term P due to a heating source is given by;

$$\rho_p c_p \frac{\partial T}{\partial t} = k\Big[\frac{1}{r^2}\frac{\partial}{\partial r}(r^2 \frac{\partial T}{\partial r})\Big] + \rho_b c_b \omega_b (T_a - T) + Q + P \tag{2.7}$$

Since, our domain is a spherical tumor mass with radius R and no effect of the applied heat is on the region surrounding the tumor, the above equation is subject to the following conditions.

Boundary Conditions:

$k\frac{\partial T}{\partial r} = 0$ when $r = 0$ and $r = R$.

Initial Condition:

The temperature at $t = 0$ is assumed to be the same as core body temperature or the arterial blood temperature T_a.

2.2 Numerical Study

Equation (2.7) on simplification gives;

$$\rho_p c_p \frac{\partial T}{\partial t} = k\Big[\frac{\partial^2 T}{\partial r^2} + \frac{2}{r}\frac{\partial T}{\partial r}\Big] + \rho_b c_b \omega_b (T_a - T) + Q + P \tag{2.8}$$

To solve equation (2.8) numerically, we use the finite-difference method (forward-difference scheme) and divide the spatial and time domains into small intervals Δr and Δt respectively, such that $r = (i-1)\cdot\Delta r$, $(i = 1, 2, ..., \lambda)$ and t $= (j-1)\cdot\Delta t$, $(j = 1, 2, ..., \mu)$, and we denote the temperature at the nodal point $i \cdot \Delta r$ at the time $j \cdot \Delta t$ by $T_{i,j}$.

Equation (2.8) for $i = 2, ..., \lambda$ and $j = 1, 2, ..., \mu$ reduces to;

$$\rho_p c_p \frac{T_{i,j+1} - T_{i,j}}{\Delta t} = k\Big[\frac{2}{i-1}\frac{T_{i+1,j} - 2T_{i,j} + T_{i-1,j}}{\Delta r^2} + \frac{T_{i+1,j} - T_{i,j}}{\Delta r^2}\Big] + \rho_b c_b \omega_b (T_a - T_{i,j}) + Q_{i,j} + P_{i,j} \tag{2.9}$$

where $P_{i,j}$ is the power dissipated by the magnetic fluid heat source at $(i,j)^{th}$ nodal point.

Equation (2.9) on simplification gives;

$$T_{i,j+1} = T_{i,j} + \frac{k\Delta t}{\rho_p c_p \Delta r^2}\Big[\Big(1 - \frac{2}{i-1}\Big)(T_{i+1,j} - T_{i,j}) - (T_{i,j} - T_{i-1,j})\Big] + \frac{\rho_b c_b \omega_b \Delta t}{\rho_p c_p}(T_a - T_{i,j}) + \frac{\Delta t}{\rho_p c_p}(Q_{i,j} + P_{i,j}) \tag{2.10}$$

for $i = 2, 3, ...\lambda$ and $j = 1, 2, ..., \mu$.

The term $\frac{\Delta t}{\rho_p c_p} Q_{i,j} \simeq 0$ (as $Q_{ij} = 7079.3\text{kgm}^{-3}$ for all i, j, hence $\frac{\Delta t}{\rho_p c_p} Q_{i,j} = 0.001\Delta t \simeq 0$) and has a negligible effect on the temperature $T_{i,j}$ and hence we neglect this term.

Thus we have;

$$T_{i,j+1} = T_{i,j} + \frac{k\Delta t}{\rho_p c_p \Delta r^2}\left[\left(1 - \frac{2}{i-1}\right)(T_{i+1,j} - T_{i,j}) - (T_{i,j} - T_{i-1,j})\right] + \frac{\rho_b c_b \omega_b \Delta t}{\rho_p c_p}(T_a - T_{i,j}) + \frac{\Delta t}{\rho_p c_p}(P_{i,j}) \tag{2.11}$$

which gives the temperature T at time any time t and radius r such that $0 < r < R$.

For $r = 0$, we have $i = 1$ which makes the RHS of equation (2.11) undefined. In this case we apply L'Hopitals rule to the term $\frac{2}{r}\frac{\partial T}{\partial r}$, having r in the denominator, of equation (2.8) as given below;

$$\lim_{r\to 0} \frac{2}{r}\frac{\partial T}{\partial r} = \lim_{r\to 0}\left[2\left(\frac{\partial T/\partial r}{r}\right)\right] = \lim_{r\to 0}\left[2\left(\frac{\partial^2 T}{\partial r^2}\right)\right] \tag{2.12}$$

Hence, the discretization of equation (2.8) for $r = 0$, i.e., $i = 1$ using equation (2.12) is;

$$T_{1,j+1} = T_{1,j} + \frac{6k\Delta t}{\rho_p c_p}\left(\frac{T_{2,j} - T_{1,j}}{\Delta r^2}\right) + \frac{\rho_b c_b \omega_b \Delta t}{\rho_p c_p}(T_a - T_{1,j}) + \frac{\Delta t}{\rho_p c_p} P_{1,j} \tag{2.13}$$

For numerical stability of equation (2.11) and equation (2.13), the following condition [23] must be satisfied;

$$\frac{k\Delta t}{\rho_p c_p \Delta r^2} \leq 0.5 \tag{2.14}$$

Boundary Conditions:

$k\frac{\partial T}{\partial r} = 0$ when $r = 0$ and $r = R$ i.e., $k\,(T_{2,j} - T_{1,j}) = 0$, or, $T_{2,j} = T_{1,j}$ and $(T_{\lambda,j} - T_{\lambda-1,j}) = 0$, or, $T_{\lambda,j} = T_{\lambda-1,j}$.

Initial Condition:

The temperature at $t = 0$ is assumed to be the same as core body temperature or the arterial blood temperature T_a, i.e., $T_{i,1} = T_a$, $(i = 1, 2, \ldots, \lambda)$.

Using Boundary Condition $T_{2,j} = T_{1,j}$ in equation (2.13), we get;

$$T_{1,j+1} = T_{1,j} + \frac{\rho_b c_b \omega_b \Delta t}{\rho_p c_p}(T_a - T_{1,j}) + \frac{\Delta t}{\rho_p c_p} P_{1,j} \tag{2.15}$$

which gives the Temperature T at the center of the tumor mass at any time t.

The temperature T at various nodal points (i, j) can be represented as the 2-D mesh given in ***Figure 6*** below.

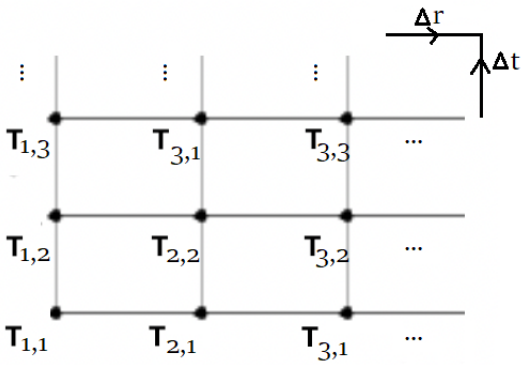

Figure 6: 2-D mesh representation of the temperature T

2.3 Integral Transform Solution

Substituting $\Phi = T_a - T$ and hence the equation (2.7) becomes;

$$\rho_p c_p \frac{\partial \Phi}{\partial t} = k\left[\frac{1}{r^2}\frac{\partial}{\partial r}\left(r^2\frac{\partial \Phi}{\partial r}\right)\right] + (\rho_b c_b \omega_b)\Phi + Q + P \tag{2.16}$$

Substituting $\Phi = \frac{\varphi}{r}$, the above equation then reduces to;

$$\frac{\rho_p c_p}{k}\frac{\partial \varphi}{\partial t} = \left[\frac{\partial^2 \varphi}{\partial r^2}\right] + (\rho_b c_b \omega_b)\frac{\varphi}{k} + \frac{r}{k}(Q+P) \tag{2.17}$$

Applying Fourier sine transform to (2.17), we have;

$$\sqrt{\frac{2}{\pi}}\int_0^\infty \frac{\rho_p c_p}{k}\frac{\partial \varphi}{\partial t}\sin(\gamma r)dr = \sqrt{\frac{2}{\pi}}\int_0^\infty \left[\frac{\partial^2 \varphi}{\partial r^2} + (\rho_b c_b \omega_b)\frac{\varphi}{k} + \frac{r}{k}(Q+P)\right]\sin(\gamma r)dr \tag{2.18}$$

which implies,

$$K\frac{\partial \bar{\varphi}}{\partial t} = -\left(\omega^2 + \gamma^2\right)\bar{\varphi} + \frac{F(\gamma)}{k} \tag{2.19}$$

where $K = \frac{\rho_p c_p}{k}$, $\omega^2 = \frac{\rho_b c_b \omega_b}{k}$, $\bar{\varphi} = \sqrt{\frac{2}{\pi}}\int_0^\infty \varphi \sin(\gamma r)\, dr$ and $F(\gamma) = \sqrt{\frac{2}{\pi}}\int_0^\infty rP(r)\sin(\gamma r)dr$ and γ is the Fourier transform variable and $\gamma \epsilon (0, \infty)$. Here, the metabolic heat generation term, Q has been omitted due to the same reason as in case of equation (2.10).

Solution of (2.19) is given by;

$$\bar{\varphi} = \left[e^{-(\omega^2+\gamma^2)t}\right]\bar{\varphi}_0 + \frac{F(\gamma)}{k\left(\omega^2+\gamma^2\right)}\left[1 - e^{-\frac{\left(\omega^2+\gamma^2\right)t}{K}}\right] \tag{2.20}$$

Assuming that $T_0 = T_a$, the arterial blood temperature we get we get $\bar{\varphi}_0 = 0$ and applying the inverse Fourier transformation $\varphi = \sqrt{\frac{2}{\pi}}\int_0^\infty \bar{\varphi}(\gamma)\sin(\gamma r)\, d\gamma$, we obtain;;

$$\varphi = \sqrt{\frac{2}{\pi}}\int_0^\infty \frac{F(\gamma)}{k\left(\omega^2+\gamma^2\right)}\left[1 - e^{-\frac{\left(\omega^2+\gamma^2\right)t}{K}}\right]\sin(\gamma r)\, d\gamma \tag{2.21}$$

Using $\frac{\varphi}{r} = \Phi$ and $\Phi - T_a = T$, we get the following equation;

$$T = T_a + \frac{1}{r}\sqrt{\frac{2}{\pi}}\int_0^\infty \frac{F(\gamma)}{k\left(\omega^2+\gamma^2\right)}\left[1 - e^{-\frac{\left(\omega^2+\gamma^2\right)t}{K}}\right]\sin(\gamma r)\, d\gamma \tag{2.22}$$

which gives the temperature profile inside the tumor mass at any time.

In our case, i.e, when the heat source is a Gaussian Distributed source we have $P = P_0\, e^{-\frac{r^2}{r_0^2}}$, $F(\gamma) = \frac{1}{2\sqrt{2}}P_0 {r_0}^3 \gamma e^{-\frac{\gamma^2 {r_0}^2}{4}}$, where r_0 is the extent of radial length covered by the magnetic fluid. The temperature inside the tumor mass at ant time t can be obtained in two cases discussed below;

Case I: Temperature For $0 < r < R$ at any time t.
Using the above relation for $F(\gamma)$ in equation (2.22), we get the following equation;

$$T = T_a + \frac{P_0 {r_0}^3}{2\sqrt{\pi}kr}\int_0^\infty \frac{\gamma e^{-\frac{\gamma^2 {r_0}^2}{4}}}{(\omega^2+\gamma^2)}\left[1 - e^{-\frac{\left(\omega^2+\gamma^2\right)t}{K}}\right]\sin(\gamma r)d\gamma \tag{2.23}$$

which gives the temperature T at any time t and raidus $0 < r < R$.

Case II: Temperature for $r = 0$ at any time t.
To obtain the temperature T at time t and $r = 0$, we substitute for $F(\gamma)$ and use L'hopital's Rule and Leibniz Rule in succession in equation (2.22). Thus at $r = 0$, we have;

$$T = T_a + \frac{P_0 {r_0}^3}{2\sqrt{\pi}k}\int_0^\infty \frac{\gamma^2 e^{-\frac{\gamma^2 {r_0}^2}{4}}}{(\omega^2+\gamma^2)}\left[1 - e^{-\frac{\left(\omega^2+\gamma^2\right)t}{K}}\right]\sin(\gamma)d\gamma \tag{2.24}$$

2.4 Steady State

Almost every steady state biological process is passes through a transient state before steady state is reached. For Steady state, i.e, as $t \to \infty$, we have;

$$T = T_a + \frac{P_0 {r_0}^3}{2\sqrt{\pi}kr} \int_0^\infty \frac{\gamma e^{-\frac{\gamma^2 {r_0}^2}{4}}}{(\omega^2 + \gamma^2)} \sin(\gamma r) d\gamma \tag{2.25}$$

which gives the steady state temperature inside the tumor mass at time t and $0 < r < R$.

Steady state temperature at $r = 0$ is obtained by letting $t \to \infty$ in (2.24) as;

$$T = T_a + \frac{P_0 {r_0}^3}{2\sqrt{\pi}k} \int_0^\infty \frac{\gamma^2 e^{-\frac{\gamma^2 {r_0}^2}{4}}}{(\omega^2 + \gamma^2)} \sin(\gamma r) d\gamma \tag{2.26}$$

3 Results

The temperature profiles in a primary hepatic cancer with a diameter of 2 cm with Gaussian source magnetic fluid at the center are analysed using the values of the physiological parameters and other numerical values characteristic of the magnetic fluid given in ***Table 1*** below. The governing equation (2.7) was solved both numerically (with spatial and time step as $3\times\ 10^{-4}$ m and $\frac{\rho_p c_p \Delta r^2}{2k}$ respectively) and analytically and obtained from (2.11), (2.15), (2.23), (2.24), (2.25) and (2.26) were plotted, clearly showing a significant agreement between the two methods used. The results obtained herein are also in agreement with the existing literature [2, 1] further validating our model.

Qty.	Value	Qty.	Value	Qty.	Value
T_a	310 K [4]	c_b	3600 J kg^{-1} K^{-1} [21]	M_d	412 kA/m [12]
k	0.57 W m^{-1} K^{-1} [4]	c_p	4180 J kg^{-1} K^{-1} [4]	K_U	9 kJ/m^{-3} [12]
ρ_p	1079 Kg m^{-3} [21]	Q	7079.3 kg m^{-3} s^{-1} [4]	D	$10.9\times\ 10^{-9}$m [12]
ρ_b	1050 Kg m^{-3} [21]	w_b	6.4×10^{-3} s^{-1} [16]	ϕ	0.003 [12]

Table 1: Various physiological and numerical values used in calculations.

The radial temperature profile of the tumor mass at various times under the Alternating Magnetic Field (AMF) and Rotating Magnetic Field (RMF) both with $H_0 = 2.0kA$ and $f = 244kHz$ with $r_0 = 3$ mm and 5 mm are are given in ***Figures* 7 - 10**.

The graphs show the temperature distribution along the radial distance of the tumor mass at different temperatures. Steady state temperatures, i.e, the maximum temperatures that are achieved and are time-independent subject to the boundary conditions of equation (2.7) have also been obtained and depicted in the graphs for the treatment under both the AMF and RMF.

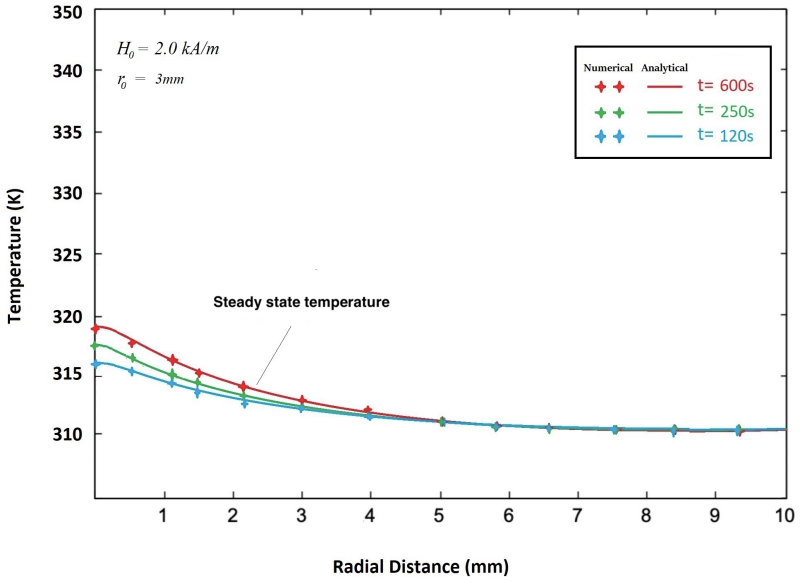

Figure 7: Temperature Profile of the tumor under AMF $r_0 = 3$ mm.

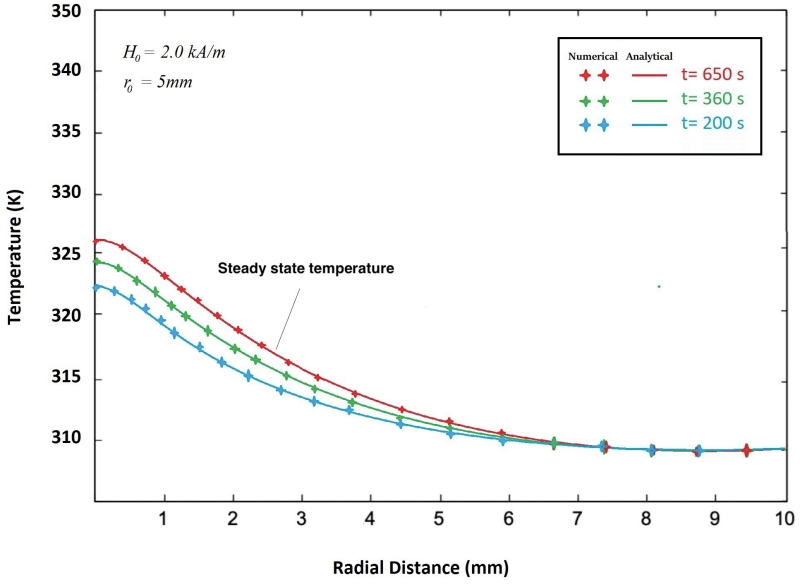

Figure 8: Temperature Profile of the tumor under AMF $r_0 = 5$ mm.

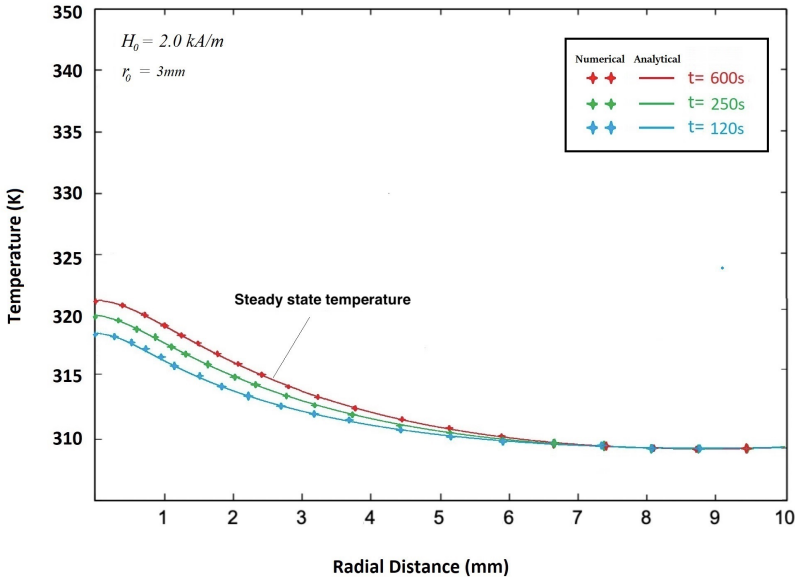

Figure 9: Temperature Profile of the tumor under RMF, $r_0 = 3$ mm.

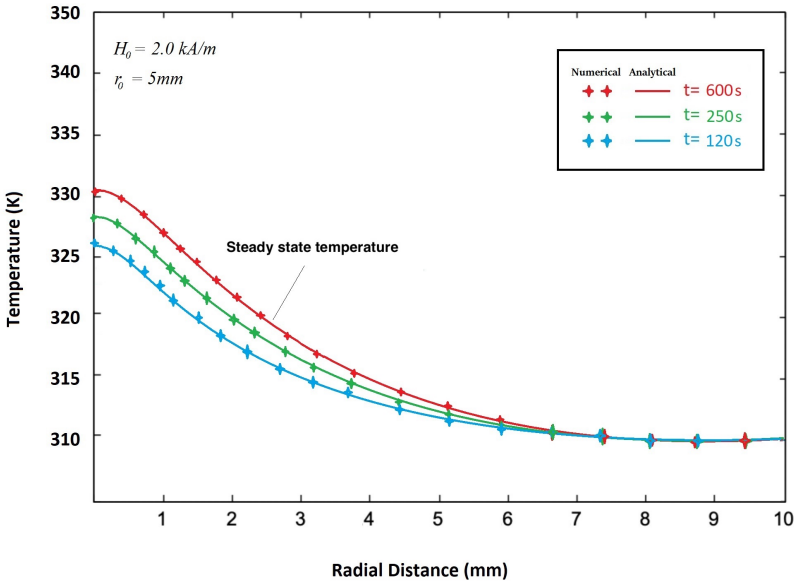

Figure 10: Temperature Profile of the tumor under RMF, $r_0 = 5$ mm.

4 Discussion and Conclusions

Magnetic Fluid Hyperthermia treatment of cancer is an emerging line of non-invasive treatment for destroying tumors in hard to reach areas and/or inoperable areas inside the body of a living organism. During the Hyperthermic treatment, it is essential that the temperature of the surrounding tissue is kept well within the cell survival limit i.e., under 315 K (42°) C. In practice, this would be ensured by using high sensitivity temperature sensors around the tumor region thus making the treatment invasive and inapplicable to areas that are inoperable. However, in this study we have used the well known Pennes' Bio Heat equation in validation with existing literature, that governs

the heat transfer in biological tissues subject to suitable boundary conditions which ensures that the temperature of healthy tissues surrounding the tumor region remains under the limit which is ensured by applying the magnetic fields only until their corresponding steady-state temperatures are achieved. We have made an attempt to mathematically study nanoparticle aided hyperthermia treatment of cancer under different types of applicated magnitic fields, i.e, Alternating Magnetic Field (AMF) and Rotating Magnetic Field (RMF). Our study shows that the identical solution of the same amount of magnetite nanoparticles under Rotating Magnetic Field (RMF) produces a greater heating effect by potentially increasing the temperature at the center of the tumor to over 330 K which is more damaging to the cancer cells compared to 325 K in case of Alternating Magnetic Field (AMF) with the same magnetic field intensity. Also, the time required to raise the temperature at the center and the rest of the tumor to above 315 K (42°C) is less in case of Rotating Magnetic Field (RMF) arrangement. The calculated steady state temperatures for Rotating Magnetic Field (RMF) were also higher than that of Alternating Magnetic Field (AMF) at same field intensities. Our findings lead to the conclusion that the application of Hyperthermia using a Rotating Magnetic Field (RMF) arrangement to heat the tumor seems to be a more promising approach which can lead to destruction of the tumor more effectively. Ongoing research has also indicated magnetic fluid consisting of Magnetite (Fe_3O_4) nanoparticles of sizes comparable to that used in our study in phosphate buffer saline to the potential candidate of Magnetic Fluid Hyperthermia owing to its high biocompatibility and stability of the solution [13].

References

[1] M. Beković, M. Trlep, M. Jesenik and A. Hamler, *A comparison of the heating effect of magnetic fluid between the alternating and rotating magnetic field*, J. Magnet. Magnetic Mater. **355** (2014), 12–17.

[2] M Beković, M. Trbušić, M. Trlep, M. Jesenik and A. Hamler, *Magnetic fluids' heating power exposed to a high-frequency rotating magnetic field*, Adv. Mater. Sci. Engin. **2018** (2018).

[3] D.K. Chatterjee, P. Diagaradjane and S. Krishnan, *Nanoparticle-mediated hyperthermia in cancer therapy*, Therapeutic Delivery **2** (2011), no. 8, 1001–1014.

[4] C.C. Chen and J.F. Kiang, *Efficacy of magnetic and capacitive hyperthermia on hepatocellular carcinoma*, IEEE Int. Symp. Anten. Prop. USNC/URSI Nat. Radio Sci. Meet., IEEE, 2018., pp. 385-386.

[5] M.G. Christiansen, C.M. Howe, D.C. Bono, D.J. Perreault and P. Anikeeva, *Practical methods for generating alternating magnetic fields for biomedical research*, Rev. Sci. Instrumen. **88** (2017), no. 8, 084301.

[6] V. Darvishi, M. Navidbakhsh and S. Amanpour, *Heat and mass transfer in the hyperthermia cancer treatment by magnetic nanoparticles*, Heat Mass Transfer **58** (2022), no. 6, 1029–1039.

[7] J.H. Dieckhoff, T. Yoshida, K. Enpuku, M. Schilling and F. Ludwig, *Homogeneous bioassays based on the manipulation of magnetic nanoparticles by rotating and alternating magnetic fields—a comparison*, IEEE Trans. Magnet. **48** (2012), no. 11, 3792-–3795.

[8] M. Galicia-Moreno, J.A. Silva-Gomez, S. Lucano-Landeros, A. Santos, H.C. Monroy-Ramirez and J. Armendariz-Borunda, *Liver cancer: Therapeutic challenges and the importance of experimental models*, Canad. J. Gastroenterology Hepatology **2021** (2021).

[9] I. Heinonen, R.M. Brothers, J. Kemppainen, J. Knuuti, K.K. Kalliokoski and C.G. Crandall, *Local heating, but not indirect whole body heating, increases human skeletal muscle blood flow*, J. Appl. Physiol. **111** (2011), no. 3, 818–824.

[10] B. Hildebrandt, P. Wust, O. Ahlers, A. Dieing, G. Sreenivasa, T. Kerner, R. Felix and H. Riess, *The cellular and molecular basis of hyperthermia*, Crit. Rev. Oncol. Hematol. **43** (2002), no. 1, 33—56.

[11] P. Ilg and M. Kröger, *Dynamics of interacting magnetic nanoparticles: effective behavior from competition between Brownian and Néel relaxation*, Phys. Chem. Chem. Phys. **22** (2020), no. 39, 22244–22259.

[12] A. Jordan, R. Scholz, P. Wust, H. Fähling, J. Krause, W. Wlodarczyk, B. Sander, Th. Vogl and R. Felix, *Effects of magnetic fluid hyperthermia (MFH) on C3H mammary carcinoma in vivo*, Int. J. Hyperthermia **13** (1997), no. 6, 587–605.

[13] R. Joshi, B.P. Singh and R.S. Ningthoujam, *Confirmation of highly stable 10 nm sized Fe3O4 nanoparticle formation at room temperature and understanding of heat-generation under AC magnetic fields for potential application in hyperthermia*, AIP Adv. **10** (2020), no. 10, 105033, .

[14] A.V. Karavaev, N.A. Gumerov, K. Papadopoulos, X. Shao, A.S. Sharma, W. Gekelman, A. Gigliotti, P. Pribyl and S. Vincena, *Generation of whistler waves by a rotating magnetic field source*, Phys. Plasmas **17** (2010), no. 1, 012102.

[15] S. Lacis, *Bending of ferrofluid droplet in rotating magnetic field*, J. Magnet. Magnet. Mater. **201** (1999), no. 1–3, 335—338.

[16] S. Maenosono and S. Saita, *Theoretical assessment of FePt nanoparticles as heating elements for magnetic hyperthermia*, IEEE Trans. Magn. **42** (2006), no. 6, 1638–1642.

[17] V.V. Mody, A. Singh and B. Wesley, *Basics of magnetic nanoparticles for their application in the field of magnetic fluid hyperthermia*, Eur. J. Nanomed. **5** (2013), no. 1, 11–21.

[18] K. Murase, J. Oonoki, H. Takata, R. Song, A. Angraini, P. Ausanai and T. Matsushita, *Simulation and experimental studies on magnetic hyperthermia with use of superparamagnetic iron oxide nanoparticles*, Radiol Phys. Technol. **4** (2011), no. 2, 194–202.

[19] L. Panawala, *Difference Between Apoptosis and Necrosis*, PEDIAA, 2017.

[20] H.H. Pennes, *Analysis of tissue and arterial blood temperature in the resting forearm*, J. Appl. Physiol. **1** (1948), 93—122.

[21] B. Radjenović, M. Sabo, L. Šoltes, M. Prnova, P. Čičak and M. Radmilović-Radjenović, *On efficacy of microwave ablation in the thermal treatment of an early-stage hepatocellular carcinoma*, Cancers **13** (2021), no. 22, 5784.

[22] R.E. Rosensweig, *Ferrohydrodynamics*, Dover, New York, 1997.

[23] G.D. Smith, *Numerical Solution of Partial Differential Equations with Exercises and Worked Solutions*, Oxford University Press, London, 1965.

[24] T. Yoshida, K. Enpuku, J. Dieckhoff, M. Schilling and F. Ludwig, *Magnetic fluid dynamics in a rotating magnetic field*, J. Appl. Phys. **111** (2012), no. 5, 053901.

[25] A. Zakinyan, O. Nechaeva and Y. Dikansky, *Motion of a deformable drop of magnetic fluid on a solid surface in a rotating magnetic field*, Experim. Thermal Fluid Sci. **39** (2012), 265–268.